# The role of organic cations in the electrochemical reduction of $CO_2$ in aprotic solvents

Jon-Marc McGregor[1], Jay T. Bender[1], Amanda S. Petersen[2], Louise Cañada[1], Jan Rossmeisl[2], Joan F. Brennecke[1], Joaquin Resasco[1*]

1. McKetta Department of Chemical Engineering, University of Texas at Austin, Austin, Texas 78712, USA
2. Department of Chemistry, University of Copenhagen, Copenhagen DK-2100, Denmark

*Corresponding Author: resasco@utexas.edu

# Abstract

The electrochemical reduction of $CO_2$ is sensitive to the microenvironment surrounding catalytic active sites. Although the impact of changing electrolyte composition on $CO_2$ reduction kinetics in aqueous electrolytes has been studied intensively, less is known about the influence of the electrochemical environment in non-aqueous solvents. Here, we present data demonstrating that organic alkyl ammonium cations influence catalytic performance in non-aqueous media and describe a physical model that rationalizes these observations. Using results from a combination of kinetic, spectroscopic, and computational techniques, we argue that the interfacial electric field present at the catalyst surface is sensitive to the molecular identity of the organic cation in the aprotic electrolyte. This is true irrespective of solvent, electrolyte ionic strength, or the supporting electrolyte counter anion. Our results suggest that changes in the interfacial field can be attributed to differences in the cation-electrode distance. Changes in the electric field strength are consequential to $CO_2R$ to CO as they modify the energetics of the kinetically relevant $CO_2$ activation step.


# Introduction

Increases in the atmospheric concentration of $CO_2$ caused by human activities threaten to cause serious environmental and societal problems. Thus, the development of low-carbon technologies that can address this issue is a pressing need. Electrochemical conversion of carbon dioxide ($CO_2R$) is such a technology, offering a means to store energy from intermittent renewable sources in the form of chemical bonds and to produce carbon-neutral fuels and chemicals.[1,2] Despite significant research efforts aimed at increasing the activity of (electro)catalysts for forming valuable products such as carbon monoxide, formic acid, ethylene, and ethanol while limiting selectivity to the parasitic hydrogen evolution reaction (HER), further advances are needed.[3,4]

Beyond modifying the composition and structure of catalytic active sites, it is now clear that changes to the environment in which the reaction occurs– including the local pH, selection of electrolyte ions, and solvent – result in significant differences in measured (electro)-catalytic activity.[5–11] For $CO_2R$, the magnitude of rate enhancements observed by changing electrolyte composition is as large as those achieved through active site modification.[12] Significant work has been done to describe the physical phenomena behind these electrolyte effects in aqueous media. These studies have focused on understanding the role of alkali metal cations, buffering anions, and electrolyte pH on the kinetics of $CO_2R$.[13–23] But far less work has been done to systematically investigate the role of the electrochemical environment in aprotic electrolytes. Despite this, aprotic electrolytes provide several attractive properties, such as high $CO_2$ solubility, the absence of acid-base equilibria that limit the concentration of dissolved $CO_2$ in water, and minimal HER reactivity.[1,24–30]

Here, we present work explaining the role of organic alkyl ammonium and phosphonium cations on the electrochemical reduction of $CO_2$ in aprotic media. We demonstrate that decreasing the size of

organic cations, by reducing the length of their alkyl chains, increases the rate of $CO_2R$ to CO on silver (Ag) surfaces irrespective of electrolyte concentration, ion pairing, and solvent identity. We attribute these effects to differences in the interfacial electric field experienced by adsorbates on the catalyst surface as the electrolyte cation size is changed. Increased interfacial field strength enhances reactivity by facilitating the kinetically relevant $CO_2$ activation step. This conclusion is built on evidence from steady-state voltammetric studies, kinetic measurements, *in-situ* vibrational spectroscopy, and *ab-initio* calculations. This model is consistent with work in aqueous systems that attribute changes in $CO_2$ reduction rates with varying alkali metal cations in the electrolyte to changes in interfacial field strength.[14,15,31,32] In contrast to aqueous systems, where changes in the interfacial field strength are ascribed to changes in the interfacial concentration of solvated alkali metal cations, for aprotic electrolytes, we attribute differences in the interfacial field strength to changes in cation-electrode distance. Our work provides fundamental insights into how electrolyte ions in aprotic media modify reaction energetics and offers new tools for controlling electrocatalytic performance beyond modifying the structure and composition of catalytic active sites.

# Results and Discussion

## Experimental Protocols for Non-Aqueous $CO_2$ Electrochemistry

To examine the role of organic cations, we measured $CO_2$ reduction rates over polycrystalline Ag catalysts in a series of aprotic electrolytes containing quaternary ammonium salts and one quaternary phosphonium salt. Tetraalkylammonium salts ($TXA^+$) are commonly used as supporting electrolytes in non-aqueous media due to their stability under reducing conditions and high solubility in organic solvents. Previous studies have reported that these tetraalkylammonium cations affect $CO_2R$ rates in water,[23] but to the best of our knowledge, a systematic description of how quaternary ammonium cations influence the $CO_2R$ reaction in aprotic media is yet to be established. To understand whether the effect of cation size was particular to one electrolyte system, we examined this phenomenon in several common organic solvents of varying polarity (i.e., acetonitrile, dimethyl sulfoxide, and propylene carbonate). Additionally, we evaluated electrolytes of different ionic strengths and varied counter anions. Lastly, to understand the impact of cation identity on $CO_2$ reduction rates, we compared the performance between aprotic electrolytes containing symmetric and asymmetric supporting electrolyte cations. Further experimental details are available in **Section S1 of the Supporting Information.**

All solvents studied were dried extensively, resulting in the water content of supporting electrolytes being confirmed to be <100 ppm through Karl Fischer Coulometry **(Table S1-S4 in Section S1.10).** The properties of these solvents and the schematic of the supporting electrolyte ion structures are described in **Table S5 and Scheme 1 (Section S2 of the Supporting Information),** respectively. Confirmation of asymmetric cation structures after synthesis was conducted using Nuclear Magnetic Resonance (NMR) Spectroscopy **(Figure S1-S7 in Section 3).**

Furthermore, all solvents and supporting electrolyte used in our study were determined to be stable under the operating potentials and timescales tested through electrochemical cycling **(Figure S8-S17 in Section S4-S6)**, post electrolysis NMR characterization **(Figure S18-S40 in Section S7)** and electrochemical window evaluation **(Figure S41 in Section S7).** Our experimental protocols resulted in complete selectivity to CO in $CO_2$-sparged electrolytes for all catalytic data reported in the paper, within experimental error (100% $\pm$ 5%) **(Figure S42-S46 in Section S8)**.

## Cation Effect on $CO_2R$ to CO with Changing Solvent Polarity

To understand the impact that tetraalkylammonium ($TXA^+$) cations of varying alkyl chain lengths have on $CO_2R$ reactivity, comparative electrochemical studies were performed in electrolytes containing tetraethylammonium ($TEA^+$), tetrapropylammonium ($TPA^+$), tetrabutylammonium ($TBA^+$), and tetrahexylammonium ($THA^+$) cations. Initial experiments were performed in acetonitrile, using 0.5 M tetraalkylammonium perchlorates as the supporting electrolyte. Acetonitrile is a commonly studied aprotic solvent for $CO_2R$, due to its low viscosity, high polarity, and wide electrochemical window.[33–36] As shown in **Figure 1a,** a systematic increase in CO generation rates, that is the partial current density to CO, was observed with decreasing alkyl chain length from $THA^+$ to $TEA^+$. This systematic increase was observed across all potentials in the range tested. In the absence of dissolved $CO_2$, minimal electrochemical response was observed, suggesting the absence of HER for these dry aprotic electrolytes **(refer to Figures S10-S12 and S15-S17 in Sections S4 and S6 of the Supporting Information)**. Consistent with this observation, steady-state activity measurements showed negligible hydrogen production **(refer to Figures S42-46 in Section S8 of the Supporting Information)**. The small currents observed in $N_2$ saturated electrolytes were also found to have no systematic dependence on cation size.

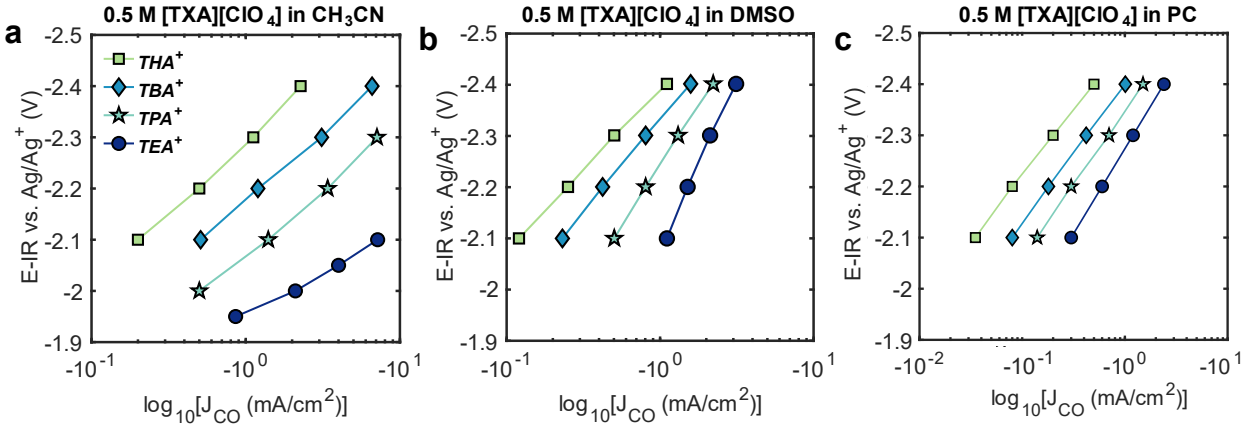


**Figure 1**: **Effect of organic cations on $CO_2R$ in aprotic electrolytes.** Tafel plots of CO formation on Ag electrodes in 0.5 M [TXA][$ClO_4$] (X=E(ethyl), P(propyl), B(butyl), H(hexyl)) in a) acetonitrile from -1.95 V to -2.4 V versus $Ag/Ag^+$ b) dimethyl sulfoxide and c) propylene carbonate from -2.1 V to -2.4 V versus $Ag/Ag^+$.

It has been previously observed that the choice of organic solvent, in addition to the supporting electrolyte, can impact rates of $CO_2R$.[37–40] To understand whether observed organic cation effects were influenced by solvent identity, parallel studies to those performed in acetonitrile ($CH_3CN$) were done in dimethyl sulfoxide (DMSO) and propylene carbonate (PC). These solvents were chosen to sample a range of dielectric strengths **(Table S5 in Section S2)** while ensuring the solubility of all supporting electrolytes. As shown in **Figure 1 b-c,** we find that irrespective of the choice of solvent tested, decreasing the alkyl chain length of quaternary ammonium cations monotonically increases CO generation rates over Ag catalysts across all potentials investigated. These results demonstrate that differences in catalytic activity with cation size are not specific to a single solvent.

## Cation Effect on $CO_2R$ to CO with Changing Electrolyte Composition

Recent work has suggested that changes in electrolyte concentration can influence the interfacial electric field experienced by adsorbates by modifying how effectively the electrochemical double layer screens surface charge.[41] Therefore, to assess whether cation effects are sensitive to double-layer charge screening, we examined the influence of varying electrolyte ionic strength. **Figure 2 and Figure S12 in Section S4 of the SI** illustrate that, at a fixed potential, shorter alkyl chains on the alkyl ammonium cations systematically increase CO generation rates in both more dilute (0.1 M) and concentrated (1 M) electrolytes, consistent with observation in 0.5 M electrolytes. In addition to these measurements in acetonitrile, consistent cation effects were observed with changing electrolyte concentration with propylene carbonate as the solvent **(Figure S16 in Section S6 of the SI).** We note that measurements for 1 M $THAClO_4$ are not shown in either solvent because this concentration exceeds the solubility limit for this electrolyte. Thus, while considering electrolyte charge screening may be important for understanding differences in activity observed with varying electrolyte concentrations for a single organic cation, these results demonstrate that the influence of changing tetraalkylammonium ($TXA^+$) cation size on CO formation is observed irrespective of electrolyte ionic strength.

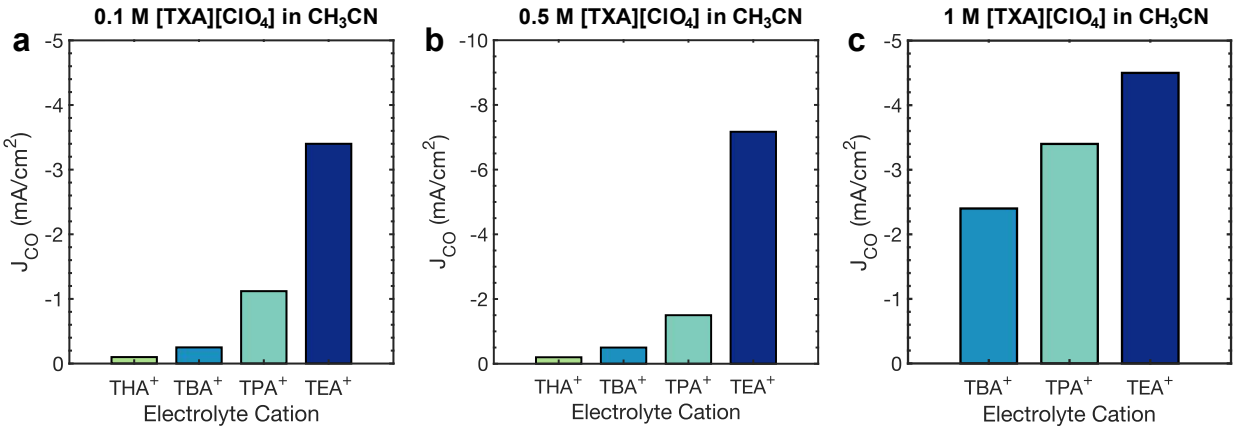


**Figure 2**: **Effect of changing electrolyte ionic strength on $CO_2R$ rates**. Partial current density to CO on Ag electrodes in a) 0.1 M b) 0.5 M and c) 1 M [TXA][$ClO_4$] (X=E(ethyl), P(propyl) B(butyl), H(hexyl)) in acetonitrile at -2.1 V versus $Ag/Ag^+$.

In addition to the effects of changing electrolyte cation, the choice of electrolyte counter anion may play a role in influencing electrocatalytic performance. In aqueous electrolytes, the identity or concentration of anions influences $CO_2R$ by buffering the local pH or acting as a proton donor.[18,20,42,43] For non-aqueous electrolytes, the role of the anion remains less understood. Recent work has attributed differences in $CO_2R$ reactivity with varying anions to the degree of ion dissociation within the electrolyte. For a fixed cation, this is dictated by both the anion identity and solvent polarity or dielectric strength.[44] These studies found that rates were insensitive to anion choice in highly polar solvents, but anion pairing appeared to influence electrochemical performance in less polar solvents. To understand whether cation effects were influenced by ion pairing, we conducted studies using tetrafluoroborate anions to compare with the results obtained with perchlorate anions presented thus far. Consistent cation-promoting effects were observed in tetrafluoroborate-containing electrolytes, with a monotonic increase in current density with decreasing cation size **(Figure 3a)**. This was true for parallel studies performed in propylene carbonate solvents as well **(Figure S17 in Section S6 of the SI)**. Under the conditions studied here, for a fixed cation in acetonitrile solutions, the choice of anion had a small effect on the overall catalytic activity **(Figure 3b and 3c)**.

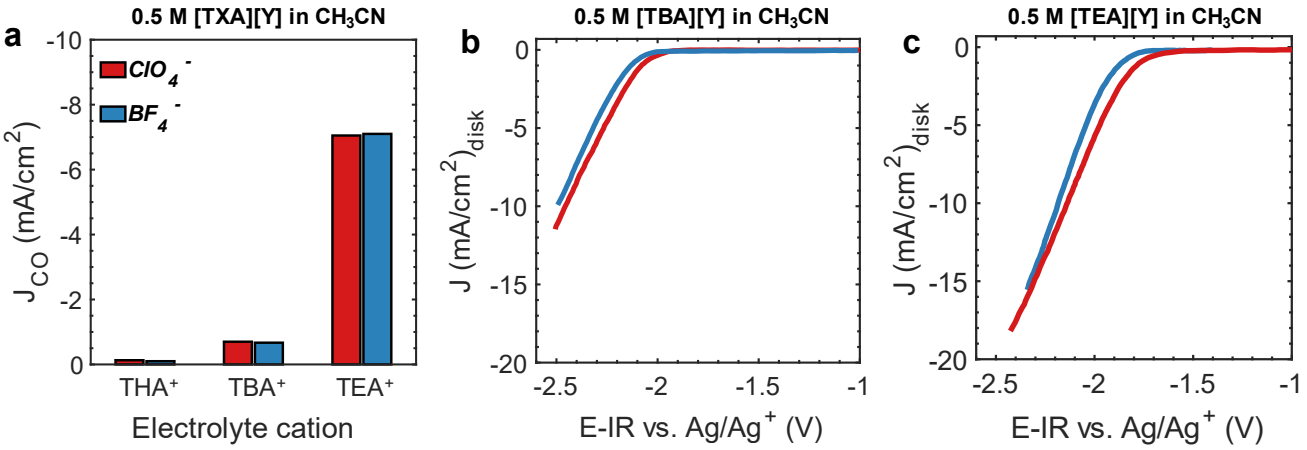


**Figure 3**: **Effect of changing electrolyte counter anion.** a) Partial current density to CO for Ag catalysts in acetonitrile containing 0.5 M [TXA][$BF_4$] (blue) and 0.5 M [TXA][$ClO_4$] (red) at -2.1 V versus $Ag/Ag^+$, b) Linear sweep voltammogram for Ag in $CO_2$ saturated acetonitrile containing 0.5 M [TBA][$ClO_4$] (blue) and 0.5 M [TBA][$BF_4$] (red), and c) Linear sweep voltammogram for Ag in $CO_2$ saturated acetonitrile containing 0.5 M [TEA][$ClO_4$] (blue) and 0.5 M [TEA][$BF_4$] (red) between potentials -1 V to -2.5 V versus $Ag/Ag^+$ . Scan rate is 50 mV/s.

## Physical Model for Understanding Cation Effects in Aprotic Electrolytes

Our results above demonstrate that the rate of $CO_2R$ to CO over Ag surfaces systematically increases with decreasing length of the alkyl chains on the tetraalkylammonium cations. This effect is observed independent of solvent choice, electrolyte concentration, or counter anion. We now describe a model that rationalizes these observations and clarifies the role of organic cations in tuning electrocatalytic rates for $CO_2R$ in non-aqueous electrolytes.

We propose that hydrophobic organic cations in aprotic media modify the interfacial electric field experienced by species adsorbed on the catalyst surface. These changes in the field modify the energy of reaction intermediates and transition states based on their polarity and polarizability. Increased interfacial fields stabilize the kinetically relevant transition state of the $CO_2$ activation step, leading to higher rates of CO generation. We propose that the strength of the interfacial electric field depends on the thickness of the electrochemical double layer, which is in turn dependent on the size of the organic cation and its separation from the negatively polarized electrode surface **(Scheme 1).** Smaller tetraalkylammonium cations, such as $TEA^+$, approach the electrode surface more closely, resulting in a steeper potential drop between the electrode and solution. This results in a larger interfacial electric field and makes these cations more effective promoters for the electrochemical reduction of $CO_2$ to CO than bulkier cations like $THA^+$ in aprotic media. Equivalently, longer alkyl chains screen the charge of the ammonium cation to a larger extent than shorter chains. This model is compatible with models proposed for alkali metal cations in aqueous electrolytes, where large, weakly solvated cations result in a higher surface charge density and greater field promotion than small, strongly hydrated cations.[15,31] To substantiate this model, we present kinetic studies that identify the elementary steps that govern the rates of $CO_2R$ over Ag surfaces in aprotic solvents. We then measure how the energetics of the rate-determining step change with cation size. Finally, we present combined spectroscopic and computational results demonstrating that changing cation size of alkylammonium cations influences the strength of the electric field experienced by adsorbates at the electrocatalyst surface.

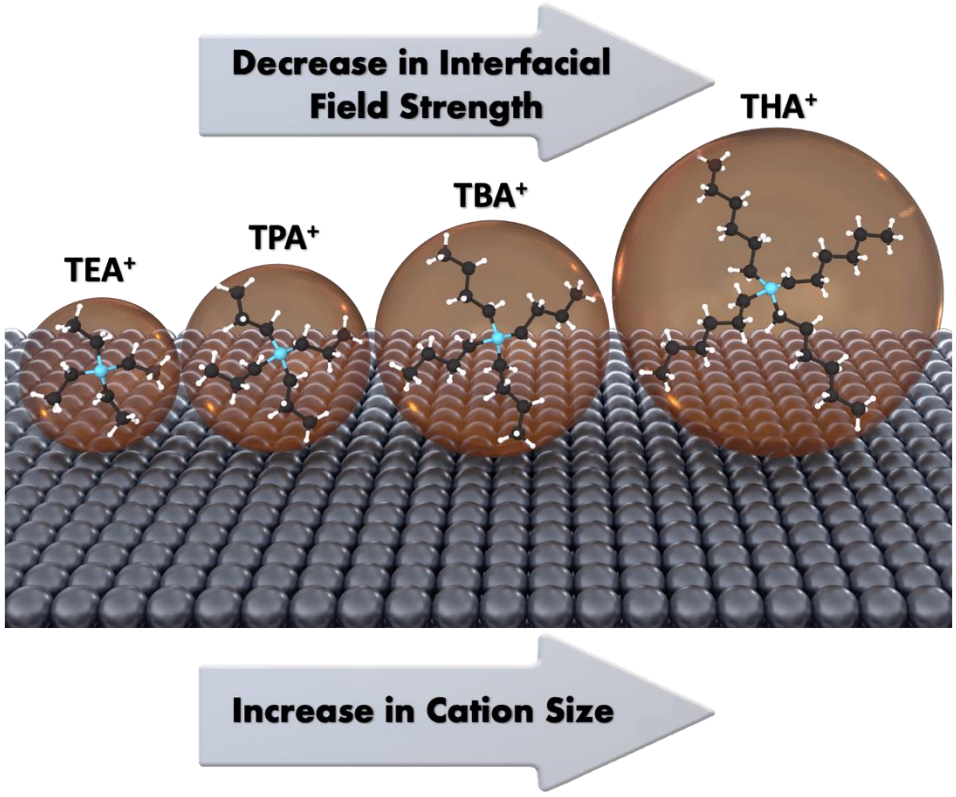


**Scheme 1: Proposed model of the impact of organic alkylammonium cations on $CO_2R$ reactivity**. Smaller cations ($TEA^+$, left) within the electric double layer are located closer to the negatively polarized Ag electrode in comparison to larger cations ($THA^+$, right). This increases the electric field intensity felt by adsorbates, facilitating $CO_2$ activation and CO formation. For simplicity, cations are shown with a spherical shape due to their symmetry.

## Probing the rate-limiting step of $CO_2R$ to CO in an aprotic medium

To understand the role of electrolyte cations, we first must identify the elementary steps that dictate rates of $CO_2R$ to CO over Ag surfaces in aprotic electrolytes. In aqueous electrolytes, CO formation is often assumed to proceed through a series of proton-coupled electron transfer (PCET) steps. We note that although the reactions below show PCET steps, water or buffering anions, rather than protons/hydronium ions, are the reactants under most experimental $CO_2R$ conditions.

$$CO_2 + H^+ + e^- + * \rightarrow COOH^* \quad (1)$$

$$COOH^* + H^+ + e^- \rightarrow CO^* + H_2O \quad (2)$$

$$CO^* \rightarrow CO + * \quad (3)$$

Although there is consensus that CO formation proceeds through a COOH* intermediate in aqueous electrolytes, it has been argued that the proton and electron transfer steps necessary for its formation are decoupled.[43,45]

$$CO_2 + e^- + * \rightarrow CO_2^{*-} \quad (4)$$

$$CO_2^{*-} + H^+ \rightarrow COOH^* \quad (5)$$

This is supported by *ab initio* calculations and the experimental observation that CO formation rates depend on an absolute potential scale (i.e., the standard hydrogen electrode) rather than the reversible hydrogen electrode scale as would be expected for a rate-determining step involving proton transfer.[46,47] It is generally agreed upon that rates of CO formation over Ag are limited by the adsorption and activation of $CO_2$, whether or not this process is proton-coupled.[48–50]

In non-aqueous media where solvents do not have easily ionizable protons, the $CO_2R$ reaction mechanism to form CO is thought to follow the sequence of elementary steps shown below.[51]

$$CO_2 + e^- + * \rightarrow {CO_2}^{*-} \quad (6)$$

$${CO_2}^{*-} + CO_2 + e^- \rightarrow CO^* + {CO_3}^{2-} \quad (7)$$

$$CO^* \rightarrow CO + * \quad (8)$$

Where (equation 6) represents the first electron transfer process (i.e., $CO_2$ activation), (equation 7) involves the disproportionation of adsorbed $CO_2$ and a solvated $CO_2$ molecule to form carbonate and adsorbed carbon monoxide, and (equation 8) describes CO desorption. We note that if the proton and electron transfer steps are decoupled in aqueous media, the $CO_2$ activation elementary steps are the same in both cases (i.e., equations 4 and 6).

To interrogate the kinetically relevant step for $CO_2R$ over Ag in aprotic solvents, $CO_2$ partial pressure-dependent measurements were conducted under conditions where mass transport is not limiting **(Figure S47 in Section S9).** Unlike in aqueous systems, changing $CO_2$ concentration in these solvents does not lead to changes in pH or buffer concentration, which can complicate kinetic analysis. As shown in **Figure 4a,** kinetic rates of CO formation exhibit a first-order dependence on $CO_2$ partial pressure. Furthermore, the $CO_2$ partial pressure dependence did not depend on cation identity ($TEA^+$, $TPA^+$, $TBA^+$, or $THA^+$), suggesting that differences in rates observed with cation size are not due to changes in the kinetically relevant step of the reaction. The first-order rate dependence is consistent with rates of CO generation limited by $CO_2$ activation, rather than carbonate formation or CO desorption **(see Section S10 of the SI for the development of the kinetic models)**. This result is chemically intuitive based on the weak binding of carbon to Ag surfaces and is consistent with the proposed rate-limiting step in aqueous electrolytes.[32,42,45,51]

Having established that CO formation rates are limited by $CO_2$ activation, we conducted temperature-dependent studies to understand how cation choice impacted the energetics of this kinetically relevant step. Measurements were taken between 5 to 45°C using an Ag rotating disk electrode for 0.1 M $TBABF_4$ and 0.1 M $TEABF_4$ in acetonitrile **(Figure S48 in Section S11; see Section S1.7 of supporting information for further experiment details). Figure 4b** illustrates the Arrhenius plot for $CO_2R$ in both electrolytes. At a fixed potential, the apparent activation energy barrier ($E_{A,\,apparent}$) decreases from 20 kJ/mol to 9 kJ/mol with decreasing alkyl chain length of the cation. Here, we reference the transition state energy to $CO_2$ in the gas phase as recommended in prior work.[8,9,52] The apparent barrier is thus lower than the true kinetic barrier as it includes stabilization by the solvent. The difference in barriers remains consistent irrespective of applied potential in the presence of $CO_2$. Both sets of kinetic experiments for $CO_2R$ in an aprotic solvent suggest that variation of cation size affects the energetics of the rate-determining step rather than influencing the identity of this elementary step. These measurements are furthermore inconsistent with cations acting as site blockers, as a change in number of accessible or highly active sites would change the intercept of the Arrhenius plot rather than its slope.

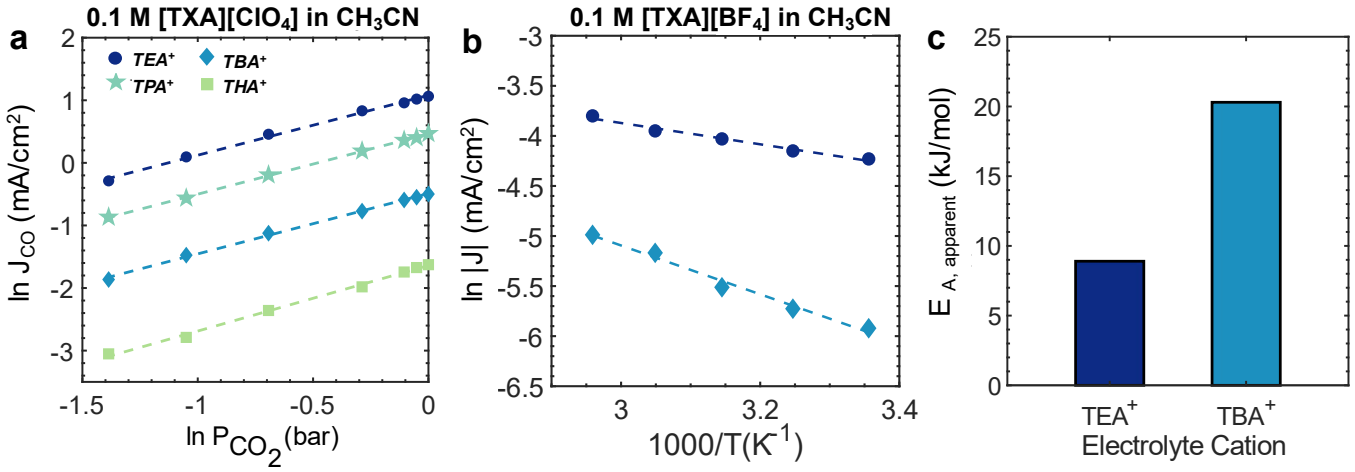

**Figure 4: Understanding the mechanism of $CO_2R$ to CO in aprotic electrolytes.** a) Dependence of CO formation rates on the partial pressure of $CO_2$ over Ag catalysts. Measurements are taken while varying choice of alkylammonium cation in an acetonitrile solution. Total inlet gas flow was kept at 1 bar and balanced with $N_2$. Measurements were taken at -2.1 V versus $Ag/Ag^+$. b) Arrhenius plot used to extract apparent activation energies for $CO_2R$ over Ag in acetonitrile at -2.1 V versus $Ag/Ag^+$. c) Calculated apparent activation energy barrier from (b) is lower for smaller cation ($TEA^+$ compared to $TBA^+$).

## Impact of interfacial electric field on $CO_2$ activation step

The results of our steady-state voltammetric, partial pressure and temperature-dependent measurements demonstrate that smaller quaternary ammonium cations lower the kinetic barrier for the $CO_2$ activation step (equation 6), facilitating CO formation. As discussed above, we attribute the changes in reaction energetics with organic cation identity to differences in the electrostatic stabilization of adsorbed $CO_2$. Field effects on catalytic reaction energetics have been implicated as a way to explain cation and pH effects in electrochemistry as well as alkali promoter effects in thermochemical catalysis.[6,15,53,54] However, the role of interfacial electric fields on $CO_2R$ in aprotic electrolytes has not been considered. The energy of an adsorbate in an electric field depends on its dipole moment and polarizability:

$$E = E_o + \mu\varepsilon - \frac{\sigma\varepsilon^2}{2} + \cdots (9)$$

Where E represents the energy of the adsorbate, $E_o$ is its energy in the absence of electric field, $\mu$ is the adsorbate's dipole moment [eÅ], $\sigma$ is its polarizability [$eÅ^2V^{-1}$] and $\varepsilon$ represents the electric field strength [$V/Å$].

Previous work by the Nørskov and Bell groups have computationally examined the impact of electric fields on $CO_2$ adsorption.[14,32] In the absence of an interfacial field, $CO_2$ adsorption is thermodynamically unfavorable on Ag surfaces.[32] As adsorbed $CO_2$ has a significant dipole, its free energy of adsorption becomes much more favorable in the presence of a negative electric field than in the absence of one. It is important to note that these calculations were done in a vacuum without proton transfer, making the conclusions independent of the solvent environment. On the basis of these studies, it has been argued that cation effects in aqueous electrolytes can be attributed to modifications of the interfacial field by electrolyte ions and consequent changes in the energetics of $CO_2$ activation.[14,15,32] The critical role of cations in facilitating this elementary step is highlighted by the complete absence of $CO_2$ reduction in aqueous electrolytes devoid of alkali metal cations.[13] Thus, there is strong precedent for the idea that interfacial fields will influence the energetics of $CO_2$ activation and CO formation over Ag catalysts in aprotic electrolytes, as suggested by our kinetic measurements.

## The influence of organic cations on the interfacial electric field

Having recognized that increases in interfacial field strength could increase rates of $CO_2R$ to CO by facilitating the activation of $CO_2$, we examined whether the choice of tetraalkylammonium cations influences this field. To do so, a combination of *in-situ* spectroscopic and computational tools was used. First, to experimentally assess changes in the interfacial field with cation size, we made use of the vibrational Stark effect employing *in-situ* electrochemical infrared spectroscopy in the attenuated total reflectance mode (ATR-IR) **(see Section S1.8 for experimental details)**. These ATR-IR measurements used CO as a probe molecule. For electrocatalytic surfaces, the Stark effect results in the observation that at fixed coverage, the stretching frequency of CO adsorbed to the electrode ($v_{CO}(\varphi)$) systematically changes in response to the applied potential.[55] This frequency shift arises from the difference in the dipole moment of the vibrational ground state and excited state $(\Delta\vec{\mu})$, with the dipole moment being larger in the elongated excited state. If the dipole is anti-parallel with the electric field, the larger dipole of the excited state leads to a greater change in its energy than that of the ground state, and thus a higher frequency of light is needed to excite this vibration. The magnitude of the change in CO stretching frequency linearly depends on the dipoles of the ground and excited states as well as the magnitude of the local electric field:[56]

$$v_{CO}(\varphi) = v_o - \Delta\vec{\mu} \cdot \vec{E}(\varphi) \quad (10)$$

where $v_o$ is the vibrational frequency $[cm^{-1}]$ of molecule in the absence of local electric field, $\Delta\vec{\mu}\ or\ \frac{dv}{d\vec{E}}$ is the probe's field free dipole moment difference known as Stark tuning rate $[cm^{-1}/(V * cm^{-1})]$ and $\vec{E}(\varphi)$ is the potential dependent interfacial electric field $[V/Å]$. Equivalently, this change in vibrational frequency with applied potential can be viewed as a change in the extent of electron donation from the metal to the CO antibonding 2π* orbital.[57]

Thus, vibrational ATR-IR spectroscopy measurements allow us to directly probe changes in electric field strength experienced by adsorbates on the catalyst surface in the presence of electrolyte cation by measuring differences in the rate of change of CO stretching frequency as a function of applied potential $\left(\frac{dv_{CO}}{d\varphi}\right)$. Here, $\frac{dv_{CO}}{d\varphi}$ is measured over a platinum (Pt) electrode in acetonitrile solutions containing quaternary cations of varied alkyl chain length **(Figure 5 a-b, Figure S49-S50 in Section S12 of the SI).** Pt is chosen as an electrode as CO coverages are known to remain fixed at monolayer coverage over the potential ranges studied.[58–62] Changes in CO coverage are known to influence vibrational frequencies through dipole-dipole interactions, thus convoluting the interpretation of Stark tuning slopes. Furthermore, the steady-state coverage of CO on Ag is very low, precluding its use as the working electrode for these spectroscopy measurements. Moreover, by independently assessing the value of $\Delta\vec{\mu}$ from experiment or computational modeling, we can determine directly how varying alkyl ammonium cation size influences interfacial field strength from equation 10 [23,63–66] or from the following equation:[67]

$$\vec{E}(\varphi) = -\frac{1}{\Delta\vec{\mu}}\frac{dv}{d\varphi}(\varphi - \varphi_o) \quad (11)$$

where $\varphi_0$ represents the potential at which the total charge on the surface is zero. It is worth noting that here no particular model of the electrochemical double layer is assumed.

In alignment with our proposed model, we found that $\frac{dv_{CO}}{d\varphi}$ monotonically increases with decreasing alkyl chain length or cation size **(Figure 5c).** These observations are in excellent agreement with prior *in-situ* spectroscopy work **(Table S5 in Section S12 of the SI)**.[55,59] Roth and Weaver further showed that these differences in $\frac{dv_{CO}}{d\varphi}$ with cation size persist with varying organic solvents at fixed ionic strength.[55] Similar observations of increasing field strength with decreasing cation size for alkylammonium cations have also been made in aqueous electrolytes.[23,68]

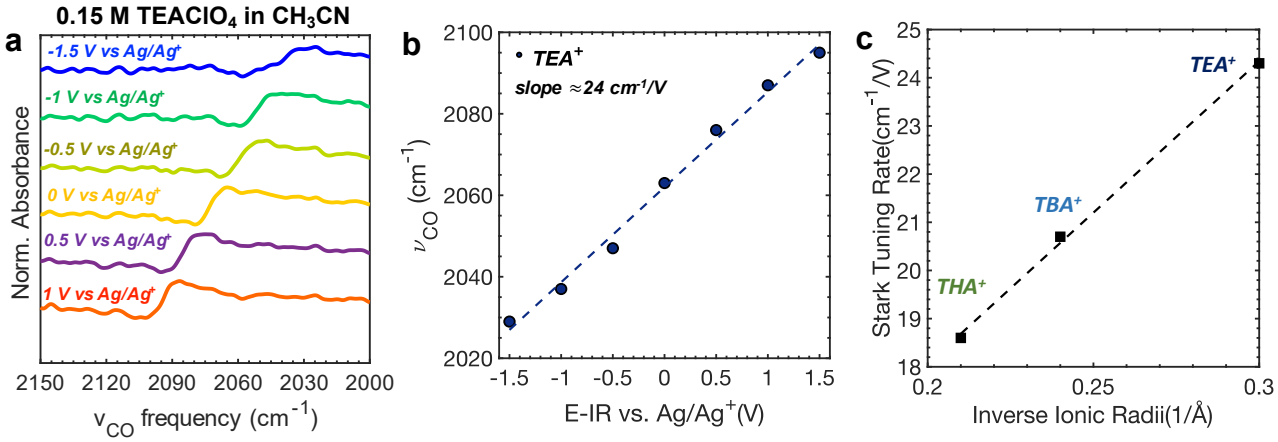


**Figure 5: Spectroscopic probes of cation-mediated field strength.** a) *In-situ* ATR IR spectra for CO adsorbed on Pt electrodes in acetonitrile containing 0.15 M $TEAClO_4$ at different applied potentials. b) The CO peak stretching frequency versus potential for the tetraethylammonium containing electrolyte. c) Linear relationship between the Stark tuning slope and the ionic radii of alkyl ammonium cations tested.

The absolute value of the field experienced by the adsorbate is likely dependent on its proximity to the cation, as previous calculations have shown these fields to be highly heterogeneous along the electrode surface.[32,69,70] As adsorbed $CO_2$ has a large dipole moment on metal surfaces, we predict that the energetics (equation 9) of the kinetically relevant $CO_2$ activation step will change monotonically with cation size. Smaller cations (e.g., $TEA^+$) will result in a greater field stabilization of the adsorbed $CO_2$, promoting its adsorption and thus the formation of CO. Overall, these spectroscopic experiments demonstrate that in support of our model, the interfacial field strength experienced by adsorbates systematically increases with decreasing alkyl chain or cation size in aprotic electrolytes.

To complement these experimental studies, density functional theory (DFT) calculations were performed to investigate differences in the adsorption geometries of the tetraalkylammonium cations ($TEA^+$, $TPA^+$, $TBA^+$, and $THA^+$) when physisorbed on a Ag (111) surface. In particular, these studies aimed to locate the equilibrium distance between the nitrogen atom of the alkylammonium cation and the metal slab [Ag- -N(Å)]. Unsurprisingly, the cation-metal distance increases monotonically with increasing chain length ($TEA^+$ <$TPA^+$<$TBA^+$<$THA^+$) **(Figure 6),** consistent with our proposed model. To understand whether these differences in the cation-metal distance are associated with

changes in the interfacial field, we performed a series of *ab initio* molecular dynamics (AIMD) simulations with the solvent molecules explicitly included. These calculations used acetonitrile as a solvent. Ammonium ($NH_4^+$) was used to represent a cation, due to the prohibitively large size of quaternary ammonium cations in the AIMD simulation. To probe the magnitude of the interfacial field, the work function was sampled at the position of the oxygen atom on adsorbed CO. To investigate how the choice of cation influences this field, the $NH_4^+$ was placed at different distances from the metal slab but allowed to relax to its preferred position in the plane parallel to the electrode **(refer to Section S1.9 of the SI for computational details)**. **Figure 6** also shows that the work function ($\phi_e$-) becomes larger and the corresponding interfacial field becomes stronger the closer the cation is to the metal surface. At large separations of the cation from the electrode, the field becomes independent of the cation position, likely due to charge screening being dominated by the solvent. This is in good agreement with prior FTIR spectroscopy work conducted by Anderson and Huang, where they observed that for higher homologues of tetraalkylammonium cations (n>6) (e.g., tetraoctylammonium perchlorate) the Stark tuning rate ($\frac{dv_{CO}}{d\varphi}$) remains unchanged in comparison with tetrahexylammonium perchlorate in acetonitrile.[59] Combined with the overlaid equilibrium positions for the quaternary ammonium cations, these AIMD calculations support our argument that an increased interfacial field strength correlates with decreasing alkyl chain length of alkyl ammonium cations.

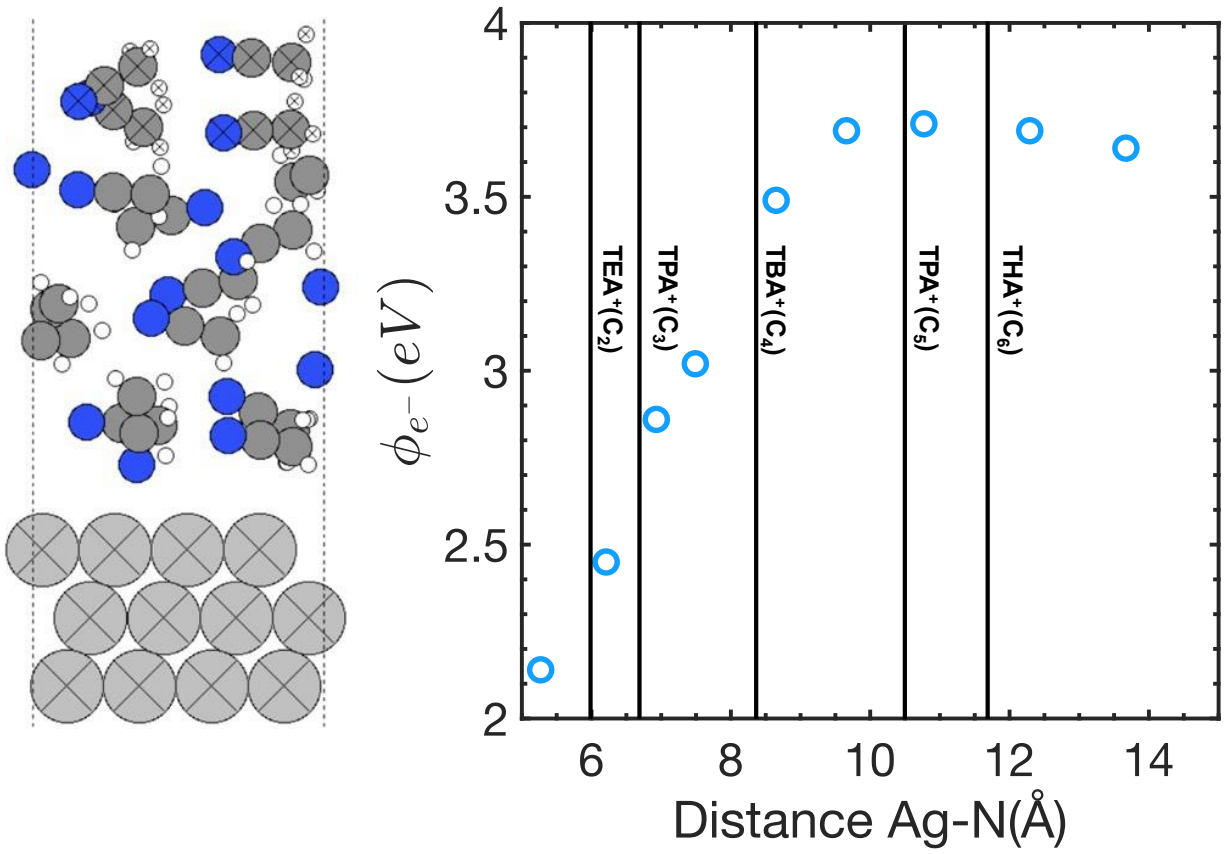


**Figure 6: Computationally probing the effect of cation size on interfacial fields.** AIMD simulation of an $NH_4^+$ ion in acetonitrile solvent. The work function ($\phi_{e^-}$) at the position of the oxygen atom of an adsorbed CO is plotted versus the separation distance between the $NH_4^+$ ion and the metal slab. Overlaid with this is the equilibrium position of quaternary ammonium cations from DFT calculations. These simulations show that the interfacial field weakens the further the organic cation ($TXA^+$) is from the metal slab.

## Cation-electrode distance is a critical parameter that influences $CO_2R$ reactivity

Finally, to examine whether the cation-electrode distance is indeed the most important parameter governing observed reactivity trends, electrochemical measurements were performed while manipulating the geometry of the quaternary cation and its central heteroatom. To investigate the influence of the cation geometry, we compared the activity of electrolytes containing symmetric tetraethyl ammonium ($TEA^+$ or $N_{2222}^+$) with those containing an asymmetric triethylhexylammonium ($N_{2226}^+$). Both electrolytes used perchlorate as the counter anion. We anticipated that the addition of one longer chain to tetraethylammonium would minimally affect its ability to approach the electrode surface **(Figure 7a)**, and, therefore, similar activity would be observed for the two cations. Consistent with this expectation, we observed nearly identical $CO_2R$ rates **(Figure 7b)** in acetonitrile electrolytes containing the two different cations. To rationalize this observation, DFT calculations were performed to examine the equilibrium separation of the $N_{2226}^+$ ion from the metal surface. The separation distance was found to be nearly identical to that of the $N_{2222}^+$ ion **(Figure S51c in Section**

**S13 of the SI)**. These calculations showed that the physisorption of the ion with the nitrogen atom closer to the surface was much more favorable than a geometry with the long alkyl chain facing the metal **(Figure S51 a,b).** AIMD simulations furthermore showed similar work functions at the two equilibrium distances for $N_{2222}^+$ and $N_{2226}^+$ **(Figure 7c)**.

Previous studies have argued that tetraalkylammonium-based cations are more effective promoters than alkyl phosphonium-based cations for $CO_2R$ in aprotic media. However, these comparisons were conducted with cations of varying geometry (e.g. butyltrimethylammonium ($N_{1114}^+$) versus triethylpentylphosphonium ($P_{2225}^+$) cations).[71] To fairly compare the promoting effects of phosphonium cations to ammonium cations and understand the impact of cation identity on $CO_2R$ performance, we compared cations of identical molecular geometry but with a different central heteroatom for $CO_2R$ ($N_{2228}^+$ versus $P_{2228}^+$) **(Figure 7d)**. As seen in **Figure 7e**, we observed nearly identical CO generation rates in electrolytes containing the two different cations. **Figure S15 in Section S6 of the SI** demonstrates that this minimal difference in activity between tetralkylphosphonium and ammonium cations occurs irrespective of solvent.

DFT calculations demonstrate that upon changing heteroatoms from nitrogen to phosphorus, the work function at the electrode-electrolyte interface is not affected **(Figure 7f),** indicating the field strength is influenced by the cation geometry rather than its molecular identity. This suggests that the role of the cation is to electrostatically modify reaction energetics, rather than participating in any direct interactions with adsorbates. DFT calculations again showed that the metal-cation distance for the most thermodynamically favored cation orientation was nearly identical in both cases **(Figure S51b in Section S13 of the SI)**. Together, these electrochemical measurements performed with varying cation geometry and composition, coupled with *ab initio* simulations, suggest that the important variable governing organic cation effects is the cation-electrode separation distance and the resulting strength of the interfacial electric field.

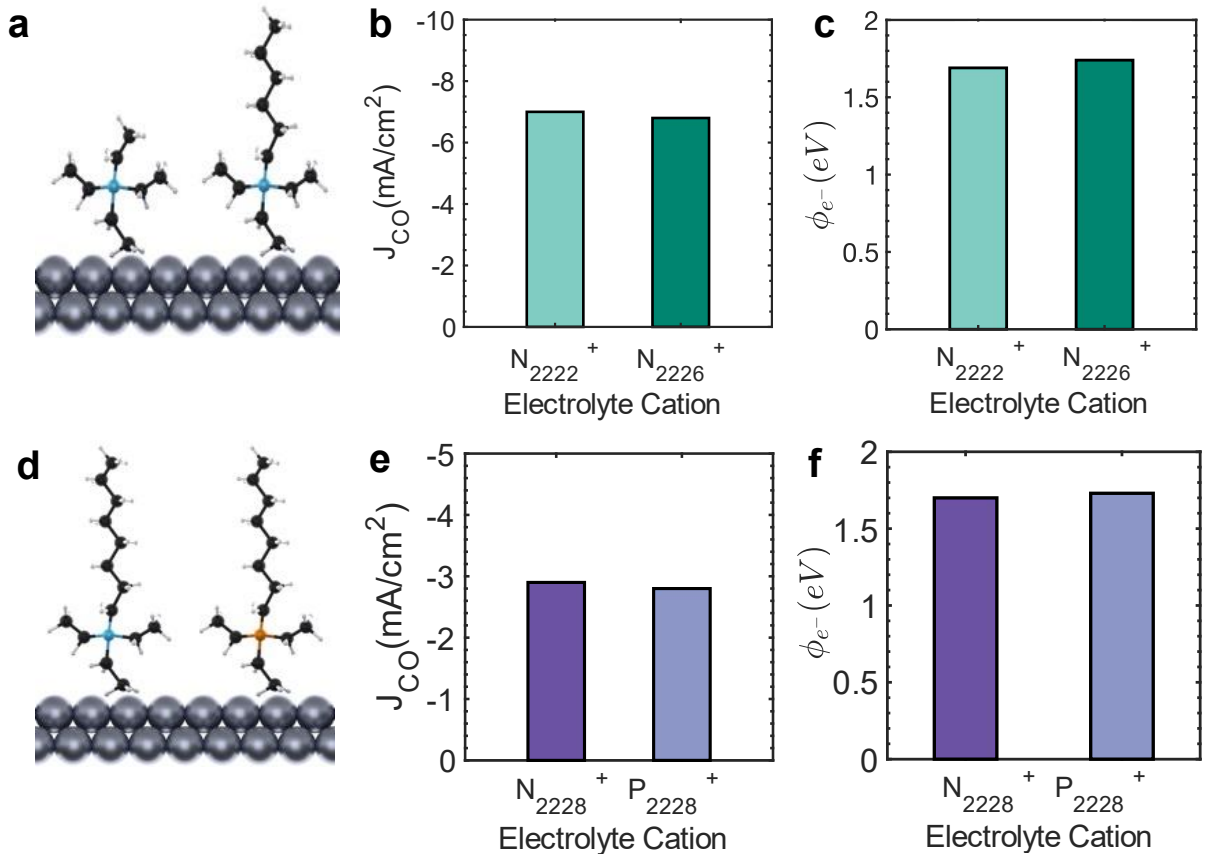


**Figure 7: Isolating the effect of metal-cation distance on $CO_2R$ reactivity.** a) Schematic illustration of the DFT calculations showing similar separation between the cation charge of single ($N_{2222}^+$) (left) and ($N_{22226}^+$) (right) at the electrode surface. b) Partial current density to CO for Ag catalysts in acetonitrile containing 0.5 M tetraethylammonium perchlorate and triethylhexylammonium perchlorate at -2.1 V versus $Ag/Ag^+$. c) Calculated work function from DFT calculations of an adsorbate on an Ag surface for an acetonitrile solvent containing an $NH_4^+$ ion at the equilibrium position of a tetraethylammonium and triethylhexylammonium cation. d) Schematic illustration of the DFT calculations showing similar separation distance between the cationic charge of $N_{2228}^+$ (left) and $P_{2228}^+$ (right) at the electrode surface. e) Partial current density to CO for Ag catalysts in acetonitrile containing 0.1 M triethyloctylphosphonium and triethyloctylammonium perchlorate at -2.1 V versus $Ag/Ag^+$. f) Calculated work function from DFT calculations of an adsorbate on an Ag surface for an acetonitrile solvent containing an $NH_4^+$ ion or a $PH_4^+$ ion at the equilibrium positions of a triethyloctylammonium and triethyloctylphosphonium cation, respectively.

## Conclusion

In this study, we have investigated the influence of tetraalkylammonium cations on $CO_2R$ over Ag surfaces in aprotic solvents and developed a physical model that describes these effects. We found that CO formation rates in an aprotic medium increase monotonically with decreasing alkyl chain length and cation size. This behavior is observed irrespective of solvent dielectric strength, electrolyte concentration, or anion pairing. Further studies demonstrated that changing properties of the cation, such as the identity of the central atom ($N_{2228}^+$ vs $P_{2228}^+$) or symmetry ($N_{2222}^+$ vs $N_{2226}^+$), minimally

impact electrocatalytic activity if they do not change the ability of the cation to approach the electrode surface. In combination with first-principles calculations, these observations suggest that the metal-cation distance is the key variable for understanding the effect of organic cations on the electrochemical reduction of $CO_2$ reduction in aprotic environments. This variable is important as it modifies the interfacial electric field experienced by adsorbates based on the thickness of the electrochemical double layer or screening of the cation charge. Based on kinetic studies, we show that this interfacial field in turn modifies the energetic landscape of the $CO_2R$ reaction in aprotic electrolytes, in particular by facilitating the kinetically relevant activation of $CO_2$. This work, using a combination of electrochemical kinetics, *in-situ* spectroscopy, and computational techniques, provides fundamental insights into the role of electric fields on catalytic reactions in aprotic solvents and how changing the reaction medium can help control these interfacial fields. Beyond deepening our understanding of catalysis in electrochemical environments, this work provides new tools for the design of selective and efficient electro-synthetic cells needed for the decarbonization of the fuels and chemicals industries.

## Author Contributions

J.M. designed and conducted all electrochemical experiments and wrote the article. J.T.B. collected all the vibrational spectroscopy data. A.S.P. performed all the computational calculations and J.Rossmeisl guided the computational efforts. L.C. synthesized and characterized the asymmetric quaternary cations. J.Resasco conceptualized the work. J.F.B and J.Resasco guided the work. All authors contributed to the discussion, review, and editing of the manuscript.

## Competing Interests

The authors declare no competing financial interest.

## Acknowledgments

J.M. gratefully acknowledges the support of ExxonMobil Corporation through the Future Leaders Academy Ph.D. Fellowship. J.F.B and J.Resasco gratefully acknowledge support from the Robert A. Welch Foundation (Grants F-1945 and F-2076, respectively). The authors would like to thank Adam Kennedy from the University of Texas at Austin Dept. of Chemistry's Glass Shop for the construction of electrochemistry glass cell components and Dr. D. Davies for assistance with graphic design. J.T.B. gratefully acknowledges the support of the National Science Foundation Graduate Research Fellowship Program (NSF-GRFP) under Grant Nos. DGE-1610403 and DGE-2137420. A.S.P and J.Rossmeisl would like to thank the Center for High Entropy Alloy (CHEAC) funded by the Danish National Research Foundation (DNRF 149) and the Villum Foundation through the Villum Center for the Science of Sustainable Fuels and Chemicals (#9444) for funding this work.

**Data availability**

All data needed to evaluate the conclusions in the paper are present in the paper and/or the Supplemental materials. Additional data related to this work are available from corresponding authors upon reasonable request.

# References


1) Hori, Y. Electrochemical $CO_2$ Reduction on Metal Electrodes. in *Modern Aspects of Electrochemistry*; Vayenas, C. G., White, R. E., Gamboa-Aldeco, M. E., Eds.; Springer: New York, NY, **2008**.

2) Stephens, I. E. L.; et al. 2022 roadmap on low temperature electrochemical $CO_2$ reduction. *J. Phys. Energy* **2022**, 4, 042003.

3) Nitopi, S.; Bertheussen, E.; Scott, S. B.; Liu, X.; Engstfeld, A. K.; Horch, S.; Seger, B.; Stephens, I. E. L.; et al. Progress and Perspectives of Electrochemical $CO_2$ Reduction on Copper in Aqueous Electrolyte. *Chem. Rev.* **2019**, *119* (12), 7610–7672.

4) Resasco, J.; Bell, A. T. Electrocatalytic $CO_2$ Reduction to Fuels: Progress and Opportunities. *Trends Chem.* **2020**, *2*, 825–836.

5) König, M.; Vaes, J.; Klemm, E.; Pant, D. Solvents and Supporting Electrolytes in the Electrocatalytic Reduction of $CO_2$. *iScience* **2019**, *19*, 135–160.

6) Govindarajan, N.; Xu, A.; Chan, K. How pH affects electrochemical processes. *Science* **2022**, *375*, 379–380.

7) Waegele, M. M.; Gunathunge, C. M.; Li, J.; Li, X. How cations affect the electric double layer and the rates and selectivity of electrocatalytic processes. *J. Chem. Phys.* **2019**, *151*, 160902.

8) Potts, D. S.; Bregante, D. T.; Adams, J. S.; Torres, C.; Flaherty, D. W. Influence of solvent structure and hydrogen bonding on catalysis at solid–liquid interfaces. *Chem. Soc. Rev.* **2021**, *50*, 12308–12337.

9) Li, G.; Wang, B.; Resasco, D. E. Water-Mediated Heterogeneously Catalyzed Reactions. *ACS Catal.* **2020**, *10*, 1294–1309.

10) Deacon-Price, C.; da Silva, A. H. M.; Santana, C. S.; Koper, M. T. M.; Garcia, A. C. *J. Phys. Chem. C* **2023**, *127*, 14518–14527.

11) Bender, J. T.; Petersen, A. S.; Østergaard, F. C.; Wood, M. A.; Heffernan, S. M. J.; Milliron, D. J.; Rossmeisl, J.; Resasco, J. *ACS Energy Lett.* **2023**, *8*, 657–665.

12) Govindarajan, N.; Kastlunger, G.; Heenen, H. H.; Chan, K. Improving the intrinsic activity of electrocatalysts for sustainable energy conversion: where are we and where can we go? *Chem. Sci.* **2022**, *13*, 14–26.

13) Monteiro, M. C. O.; Dattila, F.; Hagedoorn, B.; García-Muelas, R.; López, N.; Koper, M. T. M. Absence of $CO_2$ electroreduction on copper, gold and silver electrodes without metal cations in solution. *Nat. Catal.* **2021**, *4*, 654–662.

14) Resasco, J.; Chen, L. D.; Clark, E.; Tsai, C.; Hahn, C.; Jaramillo, T. F.; Chan, K.; Bell, A. T. Promoter Effects of Alkali Metal Cations on the Electrochemical Reduction of Carbon Dioxide. *J. Am. Chem. Soc.* **2017**, *139*, 11277–11287.

15) Ringe, S.; Clark, E. L.; Resasco, J.; Walton, A.; Seger, B.; Bell, A. T.; Chan, K. Understanding cation effects in electrochemical $CO_2$ reduction. *Energy Environ. Sci.* **2019**, *12*, 3001–3014.

16) Gunathunge, C. M.; Ovalle, V. J.; Waegele, M. M. Probing promoting effects of alkali cations on the reduction of CO at the aqueous electrolyte/copper interface. *Phys. Chem. Chem. Phys.* **2017**, *19*, 30166–30172.

17) Gu, J.; Liu, S.; Ni, W.; Ren, W.; Haussener, S.; Hu, X. Modulating electric field distribution by alkali cations for $CO_2$ electroreduction in strongly acidic medium. *Nat. Catal.* **2022**, *5*, 268–276.

18) Resasco, J.; Lum, Y.; Clark, E.; Zeledon, J. Z.; Bell, A. T. Effects of Anion Identity and Concentration on Electrochemical Reduction of $CO_2$. *ChemElectroChem* **2018**, *5*, 1064–1072.

19) Murata, A.; Hori, Y. Product Selectivity Affected by Cationic Species in Electrochemical Reduction of $CO_2$ and CO at a Cu Electrode. *Bull. Chem. Soc. Jpn.* **1991**, *64*, 123–127.

20) Kas, R.; Kortlever, R.; Yılmaz, H.; Koper, M. T. M.; Mul, G. Manipulating the Hydrocarbon Selectivity of Copper Nanoparticles in $CO_2$ Electroreduction by Process Conditions. *ChemElectroChem* **2015**, *2*, 354–358.

21) Marcandalli, G.; Monteiro, M. C. O.; Goyal, A.; Koper, M. T. M. Electrolyte Effects on $CO_2$ Electrochemical Reduction to CO. *Acc. Chem. Res.* **2022**, *55*, 1900–1911.

22) Ovalle, V. J.; Hsu, Y.-S.; Agrawal, N.; Janik, M. J.; Waegele, M. M. Correlating hydration free energy and specific adsorption of alkali metal cations during $CO_2$ electroreduction on Au. *Nat. Catal.* **2022**, *5*, 624–632.

23) Li, J.; Li, X.; Gunathunge, C. M.; Waegele, M. M. Hydrogen bonding steers the product selectivity of electrocatalytic CO reduction. *Proc. Natl. Acad. Sci.* **2019**, *116*, 9220–9229.

24) Haynes, L. V.; Sawyer, D. T. Electrochemistry of carbon dioxide in dimethyl sulfoxide at gold and mercury electrodes. *Anal. Chem.* **1967**, *39*, 332–338.

25) Chu, A. T.; Jung, O.; Toh, W. L.; Surendranath, Y. Organic Non-Nucleophilic Electrolyte Resists Carbonation during Selective $CO_2$ Electroreduction. *J. Am. Chem. Soc.* **2023**, *145*, 9617–9623.

26) Carbon Dioxide in Non-Aqueous Solvents at Pressures Less Than 200 KPA. Pergamon: Amsterdam, **2017**.

27) Ikeda, S.; Takagi, T.; Ito, K. Selective Formation of Formic Acid, Oxalic Acid, and Carbon Monoxide by Electrochemical Reduction of Carbon Dioxide. *Bull. Chem. Soc. Jpn.* **1987**, *60*, 2517–2522.

28) Ito, K.; Ikeda, S.; Yamauchi, N.; Iida, T.; Takagi, T. Electrochemical Reduction Products of Carbon Dioxide at Some Metallic Electrodes in Nonaqueous Electrolytes. *Bull. Chem. Soc. Jpn.* **1985**, *58*, 3027–3028.

29) Dubouis, N.; et al. The Fate of Water at the Electrochemical Interfaces: Electrochemical Behavior of Free Water Versus Coordinating Water. *J. Phys. Chem. Lett.* **2018**, *9*, 6683–6688.

30) Bagger, A.; Christensen, O.; Ivaništšev, V.; Rossmeisl, J. Catalytic $CO_2$/CO Reduction: Gas, Aqueous, and Aprotic Phases. *ACS Catal.* **2022**, *12*, 2561–2568.

31) Malkani, A. S.; Li, J.; Oliveira, N. J.; He, M.; Chang, X.; Xu, B.; Lu, Q. Understanding the electric and nonelectric field components of the cation effect on the electrochemical CO reduction reaction. *Sci. Adv.* **2020**, *6*, eabd2569.

32) Chen, L. D.; Urushihara, M.; Chan, K.; Nørskov, J. K. Electric Field Effects in Electrochemical $CO_2$ Reduction. *ACS Catal.* **2016**, *6*, 7133–7139.

33) Mairegger, T.; Li, H.; Grießer, C.; Winkler, D.; Filser, J.; Hörmann, N. G.; Reuter, K.; Kunze-Liebhäuser, J. Electroreduction of $CO_2$ in a Non-aqueous Electrolyte─The Generic Role of Acetonitrile. *ACS Catal.* **2023**, *13*, 5780–5786.

34) Foley, J. K.; Korzeniewski, C.; Pons, S. Anodic and cathodic reactions in acetonitrile/tetra- n -butylammonium tetrafluoroborate: an electrochemical and infrared spectroelectrochemical study. *Can. J. Chem.* **1988**, *66*, 201–206.

35) Figueiredo, M. C.; Ledezma-Yanez, I.; Koper, M. T. M. In Situ Spectroscopic Study of $CO_2$ Electroreduction at Copper Electrodes in Acetonitrile. *ACS Catal.* **2016**, *6*, 2382–2392.

36) Tomita, Y.; Hori, Y. Electrochemical reduction of carbon dioxide at a platinum electrode in acetonitrile-water mixtures. in *Studies in Surface Science and Catalysis* vol. 114, 581–584 (Elsevier, 1998).

37) Shi, J.; Shen, F.-x.; Shi, F.; Song, N.; Jia, Y.-J.; Hu, Y.-Q.; Li, Q.-Y.; Liu, J.-x.; Chen, T.-Y.; et al. Electrochemical reduction of $CO_2$ into CO in tetrabutylammonium perchlorate/propylene carbonate: Water effects and mechanism. *Electrochim. Acta* **2017,** 240, 114-121.

38) Berto, T. C.; Zhang, L.; Hamers, R. J.; Berry, J. F. Electrolyte Dependence of $CO_2$ Electroreduction: Tetraalkylammonium Ions Are Not Electrocatalysts. *ACS Catal.* **2015**, *5*, 703–707.

39) Cencer, M. M.; Li, C.; Agarwal, G.; Gomes Neto, R. J.; Amanchukwu, C. V.; Assary, R. S. Interactions of $CO_2$ Anion Radicals with Electrolyte Environments from First-Principles Simulations. *ACS Omega* **2022**, *7*, 18131–18138.

40) König, M.; Vaes, J.; Pant, D.; Klemm, E. Effect of Solvents on Aprotic $CO_2$ Reduction: A Study on the Role of $CO_2$ Mass Transport in the Product Selectivity between Oxalate and Carbon Monoxide. *J. Phys. Chem. C* **2023**, *127,* 18159-18166.

41) Liu, B.; Guo, W.; Gebbie, M. A. Tuning Ionic Screening To Accelerate Electrochemical $CO_2$ Reduction in Ionic Liquid Electrolytes. *ACS Catal.* **2022**, *12*, 9706–9716.

42) Wuttig, A.; Yaguchi, M.; Motobayashi, K.; Osawa, M.; Surendranath, Y. Inhibited proton transfer enhances Au-catalyzed $CO_2$-to-fuels selectivity. *Proc. Natl. Acad. Sci.* **2016**, *113,* 4585-4593.

43) Wuttig, A.; Yoon, Y.; Ryu, J.; Surendranath, Y. Bicarbonate Is Not a General Acid in Au-Catalyzed $CO_2$ Electroreduction. *J. Am. Chem. Soc.* **2017**, *139*, 17109–17113.

44) Gomes, R. J.; Birch, C.; Cencer, M. M.; Li, C.; Son, S.-B.; Bloom, I. D.; Assary, R. S.; Amanchukwu, C. V. Probing Electrolyte Influence on $CO_2$ Reduction in Aprotic Solvents. *J. Phys. Chem. C* **2022**, *126*, 13595–13606.

45) Hansen, H. A.; Varley, J. B.; Peterson, A. A.; Nørskov, J. K. Understanding Trends in the Electrocatalytic Activity of Metals and Enzymes for $CO_2$ Reduction to CO. *J. Phys. Chem. Lett.* **2013**, *4*, 388–392.

46) Ringe, S. The importance of a charge transfer descriptor for screening potential $CO_2$ reduction electrocatalysts. *Nat. Commun.* **2023**, *14*, 2598.

47) Ringe, S.; Morales-Guio, C. G.; Chen, L. D.; Fields, M.; Jaramillo, T. F.; Hahn, C.; Chan, K. Double layer charging driven carbon dioxide adsorption limits the rate of electrochemical carbon dioxide reduction on Gold. *Nat. Commun.* **2020**, *11*, 33.

48) Alsunni, Y. A.; Alherz, A. W.; Musgrave, C. B. Electrocatalytic Reduction of $CO_2$ to CO over Ag (110) and Cu (211) Modeled by Grand-Canonical Density Functional Theory. *J. Phys. Chem. C* **2021**, *125*, 23773–23783.

49) Rosen, J.; Hutchings, G. S.; Lu, Q.; Rivera, S.; Zhou, Y.; Vlachos, D. G.; Jiao, F. Mechanistic Insights into the Electrochemical Reduction of $CO_2$ to CO on Nanostructured Ag Surfaces. *ACS Catal.* **2015**, *5*, 4293–4299.

50) Clark, E. L.; Ringe, S.; Tang, M.; Walton, A.; Hahn, C.; Jaramillo, T. F.; Chan, K.; Bell, A. T. Influence of Atomic Surface Structure on the Activity of Ag for the Electrochemical Reduction of $CO_2$ to CO. *ACS Catal.* **2019**, *9*, 4006–4014.

51) Amatore, C.; Saveant, J. M. Mechanism and kinetic characteristics of the electrochemical reduction of carbon dioxide in media of low proton availability. *J. Am. Chem. Soc.* **1981**, *103*, 5021–5023.

52) Li, G.; Wang, B.; Resasco, D. E. Solvent effects on catalytic reactions and related phenomena at liquid-solid interfaces. *Surface Science Reports* **2021**, *76*, 100541.

53) Linic, S.; Barteau, M. A. On the Mechanism of Cs Promotion in Ethylene Epoxidation on Ag. *J. Am. Chem. Soc.* **2004**, *126*, 8086–8087.

54) Lang, N. D.; Holloway, S.; Nørskov, J. K. Electrostatic adsorbate-adsorbate interactions: The poisoning and promotion of the molecular adsorption reaction. *Surface Science* **1985**, *150*, 24–38.

55) Roth, J. D.; Weaver, M. J. Role of double-layer cation on the potential-dependent stretching frequencies and binding geometries of carbon monoxide at platinum-nonaqueous interfaces. *Langmuir* **1992**, *8*, 1451–1458.

56) Fried, S. D.; Boxer, S. G. Measuring Electric Fields and Noncovalent Interactions Using the Vibrational Stark Effect. *Acc. Chem. Res.* **2015**, *48*, 998–1006.

57) Lambert, D. K. Vibrational Stark Effect of CO on Ni (100), and CO in the Aqueous Double Layer: Experiment, Theory, and Models. *J. Chem. Phys.* **1988**, *89*, 3847–3860.

58) Cuesta, A. Measurement of the surface charge density of CO-saturated Pt(111) electrodes as a function of potential: the potential of zero charge of Pt(111). *Surface Science* **2004**, *572*, 11–22.

59) Anderson, M. R.; Huang, J. The Influence of Cation Size upon the Infrared Spectrum of Carbon Monoxide Adsorbed on Platinum Electrodes. *J. Electroanal. Chem. Interfacial Electrochem.* **1991**, *318*, 335–347.

60) Tao, F.; Dag, S.; Wang, L.-W.; Liu, Z.; Butcher, D. R.; Bluhm, H.; Salmeron, M.; Somorjai, G. A. Break-Up of Stepped Platinum Catalyst Surfaces by High CO Coverage. *Science* **2010**, *327*, 850–853.

61) Mamatkulov, M.; Filhol, J.-S. An ab initio study of electrochemical vs. electromechanical properties: the case of CO adsorbed on a Pt(111) surface. *Phys. Chem. Chem. Phys.* **2011**, *13*, 7675.

62) Dimakis, N.; Navarro, N. E.; Mion, T.; Smotkin, E. S. Carbon Monoxide Adsorption Coverage Study on Platinum and Ruthenium Surfaces. *J. Phys. Chem. C* **2014**, *118*, 11711–11722.

63) Suydam, I. T.; Boxer, S. G. Vibrational Stark Effects Calibrate the Sensitivity of Vibrational Probes for Electric Fields in Proteins. *Biochemistry* **2003**, *42*, 12050–12055.

64) Clark, M. L.; Ge, A.; Videla, P. E.; Rudshteyn, B.; Miller, C. J.; Song, J.; Batista, V. S.; Lian, T.; Kubiak, C. P. $CO_2$ Reduction Catalysts on Gold Electrode Surfaces Influenced by Large Electric Fields. *J. Am. Chem. Soc.* **2018**, *140*, 17643-17655.

65) Staffa, J. K.; Lorenz, L.; Stolarski, M.; Murgida, D. H.; Zebger, I.; Utesch, T.; Kozuch, J.; Hildebrandt, P. Determination of the Local Electric Field at Au/SAM Interfaces Using the Vibrational Stark Effect. *J. Phys. Chem. C* **2017**, *121,* 22274-22285.

66) Ge, A.; Videla, P. E.; Lee, G. L.; Rudshteyn, B.; Song, J.; Kubiak, C. P.; Batista, V. S.; Lian, T. Interfacial Structure and Electric Field Probed by in Situ Electrochemical Vibrational Stark Effect Spectroscopy and Computational Modeling. *J. Phys. Chem. C* **2017**, *121,* 18674-18682.

67) Bhattacharyya, D.; Videla, P. E.; Cattaneo, M.; Batista, V. S.; Lian, T.; Kubiak, C. P. Vibrational Stark Shift Spectroscopy of Catalysts under the Influence of Electric Fields at Electrode–Solution Interfaces. *Chem. Sci.* **2021**, *12,* 10131–10149.

68) Zhao, K.; Yu, H.; Xiong, H.; Lu, Q.; Gao, Y. Q.; Xu, B. Action at a Distance: Organic Cation Induced Long Range Organization of Interfacial Water Enhances Hydrogen Evolution and Oxidation Kinetics. *Chem. Sci.* **2023**, *14,* 11076–11087.

69) Montoya, J. H.; Shi, C.; Chan, K.; Nørskov, J. K. Theoretical Insights into a CO Dimerization Mechanism in $CO_2$ Electroreduction. *J. Phys. Chem. Lett.* **2015**, *6*, 2032–2037.

70) Gauthier, J. A.; Ringe, S.; Dickens, C. F.; Garza, A. J.; Bell, A. T.; Head-Gordon, M.; Nørskov, J. K.; Chan, K. Challenges in Modeling Electrochemical Reaction Energetics with Polarizable Continuum Models. *ACS Catal.* **2019**, *9,* 920-931.

71) Zhao, S.-F.; Horne, M.; Bond, A. M.; Zhang, J. Is the Imidazolium Cation a Unique Promoter for Electrocatalytic Reduction of Carbon Dioxide? *J. Phys. Chem. C* **2016**, *120*, 23989–24001.